TASK QUARTERLY 14 No 3, 283–295

LES OF CONVERGING-DIVERGING CHANNEL FLOW WITH SEPARATION

ŁUKASZ KUBAN, WITOLD ELSNER
AND ARTUR TYLISZCZAK

Czestochowa University of Technology,
Institute of Thermal Machinery,
Al. Armii Krajowej 21, 42-200 Częstochowa, Poland
{kuban, welsner, tyliszczak}@imc.pcz.czest.pl

(Received 16 August 2010; revised manuscript received 9 October 2010)

Abstract: The paper presents the results of LES simulation of two different turbulent channels with inlet conditions corresponding to the Reynolds number $\mathrm{Re}_\tau = 395$. In both cases a varying pressure gradient was obtained by an adequate curvature of one of the walls. The first case is treated as a benchmark and is used to validate the numerical procedure. This case is characterized by the same cross-section area at the inlet and outlet and a bump of a smooth profile located on one of the walls designed to be identical to the one used in the experiment conducted at Laboratorie de Mecanique de Lille (LML) (Marquillie *et al.*, 2008). The second case corresponds to the geometry which reproduces the real geometry of the turbomachinery test section of the Czestochowa University of Technology. The test section was created in such a way as to produce the pressure gradient which would correspond to the conditions present in the axial compressor blade channel. The shape of both channels produced initially favorable (FPG) and then adverse pressure gradients (APG), and in this way created conditions for boundary layer separation. Due to a reverse flow where the turbulence transport is dictated by the dynamics of the large-scale eddies such a case is well suited to demonstrate predictive features of the LES technique.

Keywords: LES, turbulent boundary layer, separation, channel flow, pressure gradient

1. Introduction

The large eddy simulation technique is increasingly used as a tool to model such problems like nonequilibrium, three-dimensional flows, relaminarizing, re-transitioning boundary layers and massively separated flows. The main limitation of LES appears to be in the application for a wall-bounded flow. In case when the near wall region needs to be resolved, the grid must be proportional to the size of inner-layer eddies, which is strongly Reynolds number dependent. A lot of effort has been put into development of this technique in order to reduce its computational cost.

The proper solution of the near wall flow depends, inter alia, on the subgrid model applied. One of the important tasks is to take into account subgrid-scale dissipation at smallest scales, which leads to significant improvements of the isotropic turbulence description. The accuracy of the LES solution depends strongly on two main sources of errors, introduced by the discretization method and by the subgrid-scale model. Meyers *et al.* [1, 2] have shown that those two errors for isotropic turbulence strongly interact with one another. The subgrid-scale models applied for wall-bounded flows should posses suitable properties and especially should produce eddy viscosity with correct near-wall behavior. The properties of the models have been often studied based on such classical benchmarks as the periodic channel flow [3]. The main advantage of such a case is a simple geometry, which diminishes the influence of numerical errors leaving the accuracy to the subgrid-scale model.

This last conclusion is not valid for a more complex geometry, with velocity gradients and separation. The boundary layer flow around aircraft is responsible for more than half of the drag. A further increase in the drag is present for high-lift configurations with regions of a strong adverse pressure gradient, with possible separation. This requires that predictive models should be improved and it was one of the reasons behind the establishing of the joint EU project called WALLTURB.

Recently, turbulent flows with an adverse pressure gradient have been the subject of extensive research. As early as in 1998 Wu *et al.* [4] performed the LES simulation of a flow over a two-dimensional bump with a dynamic eddy viscosity model for a range of grid resolutions with a second order spatial discretization scheme. Their prediction of the mean flow and turbulent intensities were found to be in good agreement with the measurements of Webster [5]. On the other hand they have found a great discrepancy occurring in the prediction of peak shear stress levels along the rear bump surface. The same geometry has been investigated by El-Askary [6] using LES and RANS models with a second order spatial accuracy. Both LES and RANS models have reasonably predicted the flow mean velocities, except in the adverse pressure gradient region. In 2008 Marquillie *et al.* [7] performed a DNS calculation of a channel with one curved surface for the Reynolds number $\mathrm{Re}_\tau = 395$ based on the friction velocity and the boundary layer thickness. For the curved surface they obtained a thin separation bubble with a reversal flow fraction.

The objective of this work was to perform a validation of the high-order computational code against an LML test case (DNS results) and then to apply this code to the geometry corresponding to the turbomachinery conditions. For this purpose the role of the subgrid model and mesh density on the solution were considered. The adopted test cases could be regarded as useful engineering test cases because they allowed demonstrating the predictive features of LES for simulation of an APG flow with and without wall curvature.

2. Numerical procedure

The incompressible flow is governed by the continuity equation and the Navier-Stokes equations which in a non-dimensional form in a contest of LES are given as:

$$\frac{\partial \bar{u}_j}{\partial x_j} = 0 \tag{1}$$

$$\frac{\partial \bar{u}_i}{\partial t} + \frac{\partial \bar{u}_i \bar{u}_j}{\partial x_j} = -\frac{\partial \bar{p}}{\partial x_i} + \frac{\partial}{\partial x_j}\left(\frac{1}{\mathrm{Re}_\tau}\left(\frac{\partial \bar{u}_i}{\partial x_j} + \frac{\partial \bar{u}_j}{\partial x_i}\right)\right) + \tau_{ij} \tag{2}$$

where the $(\bar{\cdot})$ symbol stands for the filtered variable obtained by convolution of the filter function (filter kernel) G with the velocity and pressure, *i.e.* u_i or p. The term τ_{ij} is the so-called subgrid stress tensor defined as:

$$\tau_{ij} = \frac{\partial}{\partial x_j}(\bar{u}_i \bar{u}_j - \overline{u_i u_j}) \tag{3}$$

The subgrid stress tensor has to be modeled because of the unknown term $\overline{u_i u_j}$. One of the most common closures is the Smagorinsky model which assumes that the subgrid stress tensor can be expressed as:

$$\tau_{ij} = 2\nu_T \bar{S}_{ij} + 1/3\tau_{ll}\delta_{ij} \tag{4}$$

where the symbol ν_T is the subgrid viscosity and S_{ij} denotes the deformation tensor computed based on the filtered velocity field:

$$\bar{S}_{ij} = \frac{1}{2}\left(\frac{\partial \bar{u}_i}{\partial x_j} + \frac{\partial \bar{u}_j}{\partial x_i}\right) \tag{5}$$

Using the Smagorinsky model the subgrid viscosity is defined as:

$$\nu_T = (\Delta C_s)^2 \sqrt{2\bar{S}_{ij}\bar{S}_{ij}} \cdot \mathcal{D} \tag{6}$$

Since the eddy-viscosity in the classical Smagorinsky model is not properly scaled near the wall, the damping function $\mathcal{D}$ similar to the van Driest damping formula was used. The function was defined as $\mathcal{D} = \left(1 - exp\left(\frac{-|y^+|}{26}\right)\right)^3$.

An interesting alternative to the Smagorinsky model is the Wall Adapting Local Eddy Viscosity (WALE) model [8], which is based on the square of the velocity gradient tensor and accounts for the effects of both the strain and the rotation rate to obtain the local eddy-viscosity. As it is based, by definition, on local quantities the model is suitable for simulation of complex geometries. Additionally, it recovers the proper near-wall scaling for the eddy-viscosity without requiring a dynamic procedure. In the WALE model the eddy viscosity is modeled by:

$$\nu_T = (\Delta C_w)^2 \frac{(S^d_{ij}S^d_{ij})^{3/2}}{(\bar{S}_{ij}\bar{S}_{ij})^{5/2} + (S^d_{ij}S^d_{ij})^{5/4}} \tag{7}$$

Simulations were performed using the in-house code SAILOR-WALL. The code relies on the projection method for the pressure-velocity coupling [9]. The time integration was performed using the Adams-Bashforth/Adams-Multon predictor-corrector scheme. The spatial derivatives were approximated by a high-order

compact scheme [10] in streamwise and wall normal directions and a Fourier approximation in the spanwise direction. The high-order discretization allows for coarsening of the grid and in this way decreasing the computational cost. The simulations were performed on structured mesh. A mapping procedure from physical to computational domain had to be applied in order to reproduce the shape of a curved wall [7]. The inlet boundary conditions were generated for each time step from a precursor LES of a flat channel flow at the same Reynolds number. At the outlet the convective type of boundary conditions was applied in the following form:

$$\frac{\partial u}{\partial t} + u_c \frac{\partial u}{\partial n} = 0 \tag{8}$$

where u_c is the convection velocity and $\frac{\partial u}{\partial n}$ is the derivative normal to boundary.

3. Results

3.1. LML test case

The computational domain corresponds to the one used in experiments conducted in the wind tunnel of Laboratorie de Mecanique de Lille at a high Reynolds number. Marquille *et al.* [7] performed DNS calculations of this test case for the Reynolds number $\mathrm{Re}_\tau = 395$. A spatial resolution for the DNS simulation was $1536 \times 257 \times 384$. This test case was used as a benchmark for the LES procedure validation.

The computational domain is presented in Figure 1. The domain is 4π units long, 2π units wide in the spanwise direction and has two units of high at the inlet. The origin of the coordinate system is located at the top of the bump which is 3.7 units downstream from the inlet. The simulation parameters are summarized in Table 1. In the paper the statistics of LES with two different subgrid models applied for coarse and fine mesh were compared.

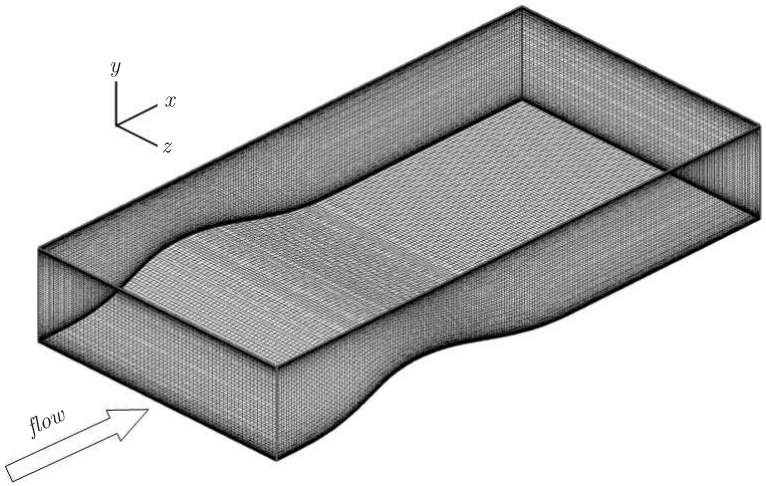

Figure 1. The computational domain of the LML test case

Table 1. Parameters of the LES simulation. C_W/C_S are the constants of a subgrid scale model, N is the number of grid points

Model	Nx	Ny	Nz	C_W/C_S
SMAG	96	96	64	0.1
NONE	96	96	64	0.0
WALE	96	96	64	0.2
WALE	96	96	64	0.4
SMAG	192	96	64	0.1
NONE	192	96	64	0.0
WALE	192	96	64	0.2
WALE	192	96	64	0.4

There is no doubt that the near wall solution depends on the grid quality. The denser the applied mesh is, the smaller the scales that need to be modeled, what is a correct tendency because small-scale turbulence displays universal properties. In the following work the mesh spacing in the streamwise direction varies from $\Delta x^+ = 50.9$ to $\Delta x^+ = 25.3$ for coarse and fine mesh, respectively. In wall-normal and span-wise directions the mesh does not change for coarse and fine cases and the spacing is equal to $\Delta z^+ = 37.8$, $\Delta y^+_{\min} = 0.63$ and $\Delta y^+_{\max} = 18.74$, respectively in spanwise and wall-normal directions. The $\Delta y^+_{\min}$ and $\Delta y^+_{\max}$ correspond to the smallest and largest mesh spacing in the normal direction. In other words the mesh control volume for coarse mesh varies from $V^+_{\min} = 10.66$ to $V^+_{\max} = 33.04$ and for the fine mesh from $V^+_{\min} = 8.44$ to $V^+_{\max} = 26.17$. In the paper the main attention is devoted to the region downstream of the minimum pressure point. The results presented by Laval *et al.* [11] have shown that an increase in the resolution in the spanwise and normal direction does not lead to significantly better results at the lower wall, although it better reproduces the boundary layer behavior on the upper flat plate. That is why in the frame of the presented research it was decided to check the role of grid refinement in the streamwiese direction only. Two cases were considered with the number of grid points of 96 (named coarse mesh) and 192 (named fine mesh).

The first parameter, characterizing the test case is the pressure coefficient defined as, $C_p = \frac{P-P_0}{0.5U_0^2}$, where U_0 is the maximum velocity at the inlet. The distribution of C_p for upper and lower walls, obtained with the WALE model and compared to the DNS data are presented in Figure 2. It is seen that the pressure gradient is much stronger for the curved than for the flat wall. On the upper wall the pressure gradient is too weak to induce separation, while on the lower wall one can observe a typical diffusion zone indicating a reversal flow between $x = 0.7$ and 1.5. The LES results overlap with the DNS data, which means that the simulation captures well the main flow behavior.

An important parameter, most often used to analyze the boundary layer development, is a skin friction parameter defined as $C_f = \frac{\tau_w}{0.5\rho U_0^2}$, where τ_w is the shear stress at the wall. In Figure 3, a comparison of skin friction coefficient distribution for Smagorinsky and WALE subgrid models is presented. To reduce the size of the figures all C_f curves for the upper wall were shifted up by 0.01.

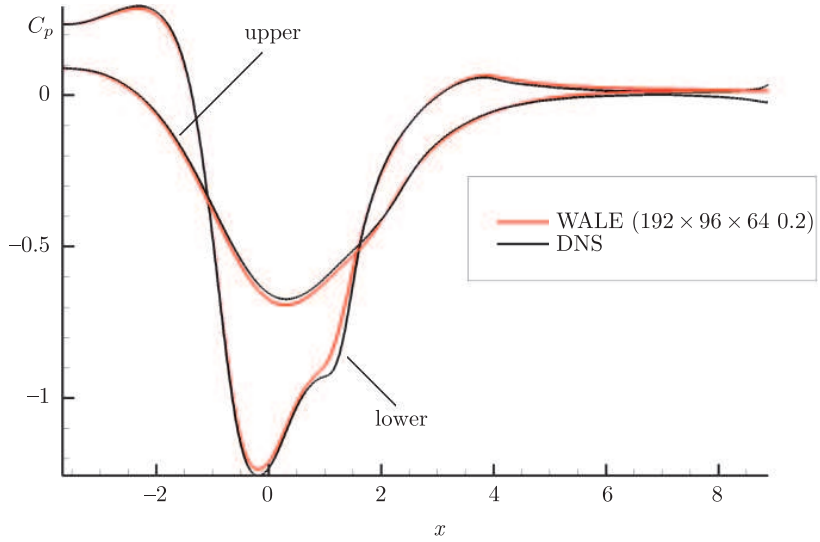

Figure 2. Pressure distribution along the domain

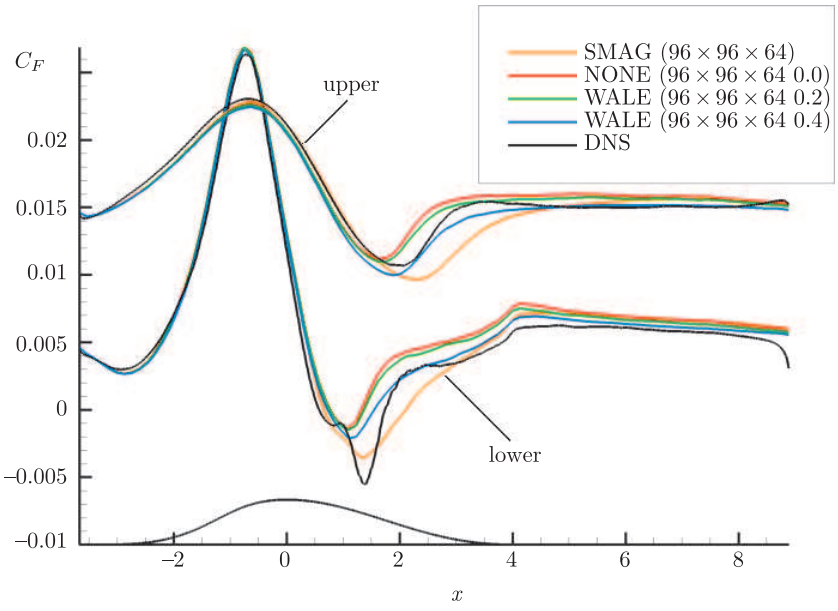

Figure 3. Comparison of skin friction coefficient for different subgrid models (Coarse mesh)

It is clear that the Smagorinsky model gives the poorest results both for the upper and lower wall. On the sloping wall of the bump the reattachment point is significantly delayed and C_f reaches the value of DNS only from $x = 4$. A similar delay is observed on the upper wall, where even minor, separation, not observed in DNS, is predicted. The reason for such flow behavior near the wall is a drawback of the Smagorinsky model, which are overdissipative and damp fluctuations near the wall. Then, there is not enough energy to close the separation bubble. The other

reason could be too low the Reynolds number. Nicoud *et al.* [8] have stated that for a low Reynolds number the cutoff filter defined by the grid spacing intersects the energy spectrum at the beginning of the dissipative range and not within the inertial range.

The role of artificial viscosity introduced by the subgrid scale model could be assessed based on the WALE results, where the constant was changed from $C_W = 0$ to $C_W = 0.4$. The WALE subgrid model with the model constant equal 0 is in fact a case without a model. It means that the subgrid kinetic energy is not dissipated by the SGS model. The role of the SGS model is hardly seen in the zero and favorable pressure gradient region, but it is apparent in the APG region, where the skin friction both on the upper and lower wall is overpredicted. On the lower wall the separation is very small and minimum C_f, indicating the center of the recirculation zone, does not match DNS at all. This may suggest that the amount of the kinetic energy generated in the APG gradient region is large and therefore, visible lack of dissipation by the SGS model is observed.

The DNS solution by Marquille *et al.* [7] shows intense generation of coherent structures in this region, probably due to a local instability in space and time resulting from local inflection points of streamwise velocity. With an increase in C_W to 0.2 some artificial viscosity is added and the C_f level changes in the direction of DNS. However, it is only for $C_W = 0.4$ that more significant improvement is observed. The same tendency is observed for the upper and lower walls.

In any case, it is clear that any of these models considered have not reproduced correct C_f levels in the recirculation zone. Probably it must have been due to a small number of grid points within this zone in the streamwise direction, therefore computations were repeated for refined mesh. By doubling the mesh size the mesh control volume decreases from $V^+_{\min} = 10.66$ to $V^+_{\min} = 8.44$ shifting the filter cutoff further in the dissipative range. The new set of C_f distributions is presented in Figure 4. Again the Smagorinsky model seems to give the worst results, and the separation bubble on the bump is twice as long as that in the DNS. It is the effect of more pronounced turbulent kinetic energy damping introduced by the SGS model. For no model case (WALE with the model constant equal 0) an improvement in comparison with the coarse mesh is observed. An increase in the model constant caused much better prediction of the C_f minimum. However, for the case with the constant equal to 0.4 it clearly overpredicts the reattachment point, but not as strongly as in the case of the Smagorinsky model. The same tendency is observed for the upper wall, where the results obtained for the model constant equal to 0.2 are in much better agreement than those for 0.4. This observation leads to the conclusion that the mesh is fine enough and the contribution of artificial viscosity (for WALE with $C_W = 0.4$) is already exaggerated.

The further detailed analysis was aimed at comparing the WALE model ($C_W = 0.2$) with the DNS results. Figure 5 shows profiles of mean axial velocity

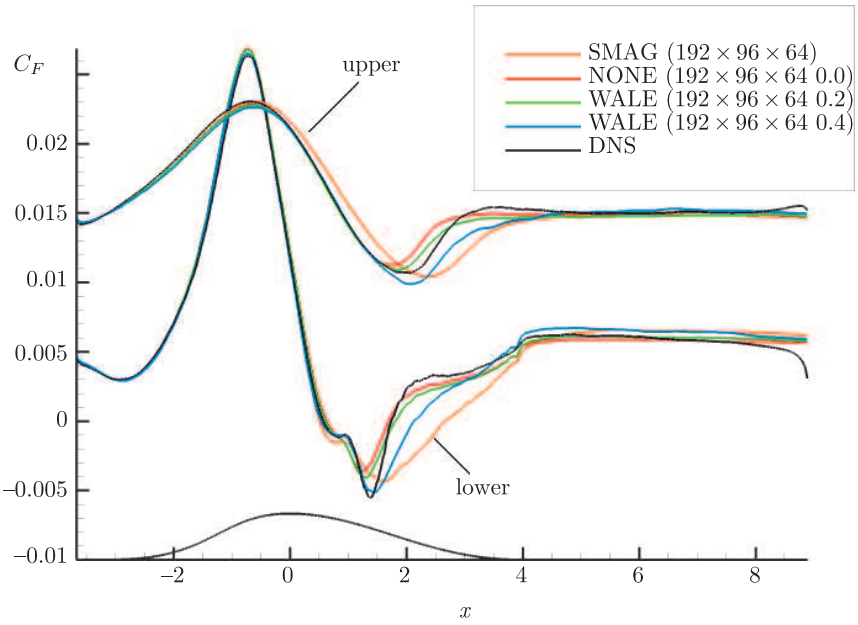

Figure 4. Comparison of skin friction coefficient for different subgrid models (Fine mesh)

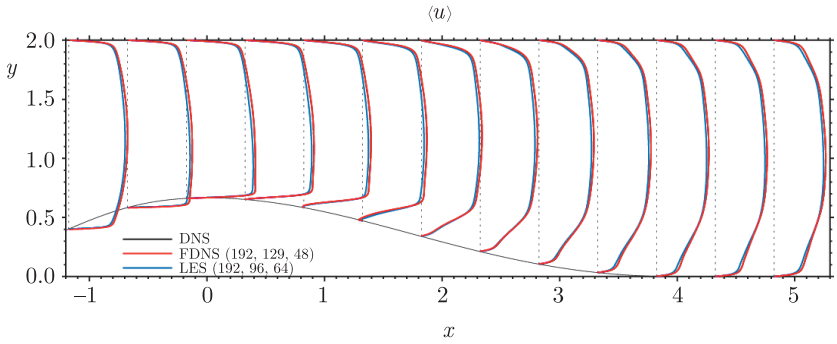

Figure 5. Mean axial velocity

together with DNS and filtered DNS solution (FDNS). The filtered solution was obtained for the similar mesh control volume size as the LES results. It is easy to see that in terms of mean axial velocity the LES solution is in excellent agreement with the FDNS results in the whole domain. The subsequent Figures 6–8 present the fluctuating velocity components. The overall LES prediction of all fluctuating components is very good. However, some discrepancies can be observed especially in the outer part of the boundary layer on the curved wall. It seems that the LES calculation predicts a slightly lower level of streamwise velocity fluctuations especially downstream of the reattachment point (Figure 6). Much better results were obtained for wall-normal and spanwise fluctuating velocity components, where the v and w profiles fit very well with the FDNS results (Figures 7–8).

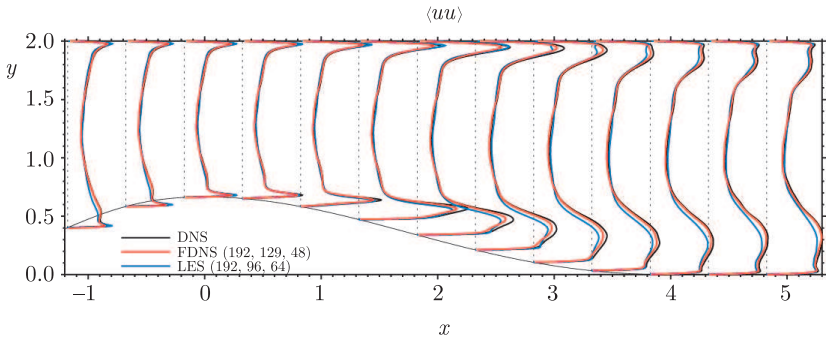

Figure 6. Fluctuating part of axial velocity component

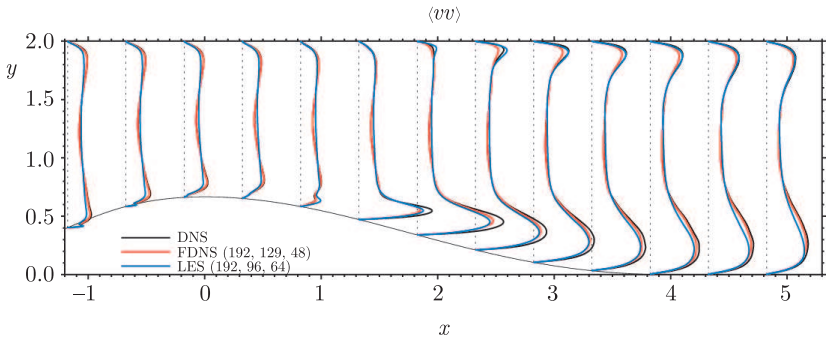

Figure 7. Fluctuating part of wall-normal velocity component

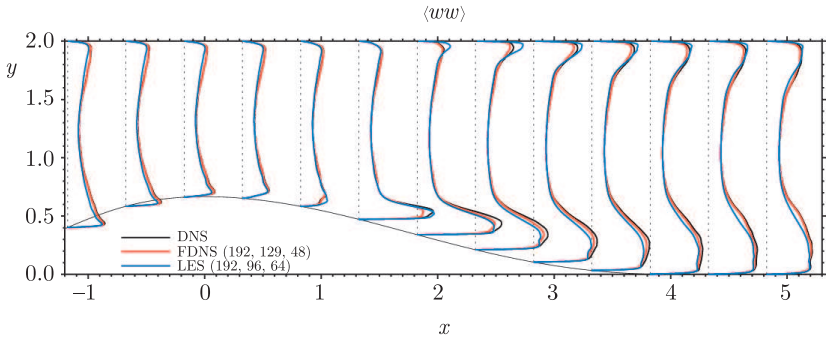

Figure 8. Fluctuating part of spanwise velocity component

One may observe that in general the LES results at the upper wall are in much better agreement with the FDNS solution than those on the lower wall. There is no difference observed for any component in the core flow.

Summing up, the application of high order approximation with relatively coarse mesh enables predicting all the details of a channel flow with a favorable and adverse pressure gradient with high quality. The role of streamwise mesh refinement was raised up, especially in the aspect of the results around the separation region. It has been shown that the quality of the results is a function of amount of artificial dissipation introduced by SGS model.

3.2. Turbomachinery test case

The second stage of the research concerns the calculation of the channel with a pressure gradient corresponding to the axial compressor blade channel gradient. In contrast to the previous case the origin of the coordinate system is located at the channel inlet. To obtain a proper pressure gradient the lower wall of the channel was properly shaped. The wall curvature and change of cross-section area produces adverse pressure gradients which creates conditions for boundary layer separation. The same test case, but for a higher Reynolds number $\mathrm{Re}_\tau = 950$ was experimentally investigated by Materny *et al.* [12]. According to the conclusions formulated in the previous section the WALE model with constant $C_W = 0.2$ seems to predict the flow behavior considerably better than the Smagorinsky model. Therefore, in this section most of the simulations were performed with the same model and the same model constant. However, for comparative study a simulation with the Smagorinsky model was also done.

The computational domain is presented in Figure 9. Similarly like for the previous case the domain has a dimension of 4π units in the streamwise direction, 2π units in the spanwise direction and 2 units of height. The same mesh as indicated in LML test case was applied, which was $192 \times 96 \times 64$ in streamwise, wall-normal and spanwise directions respectively.

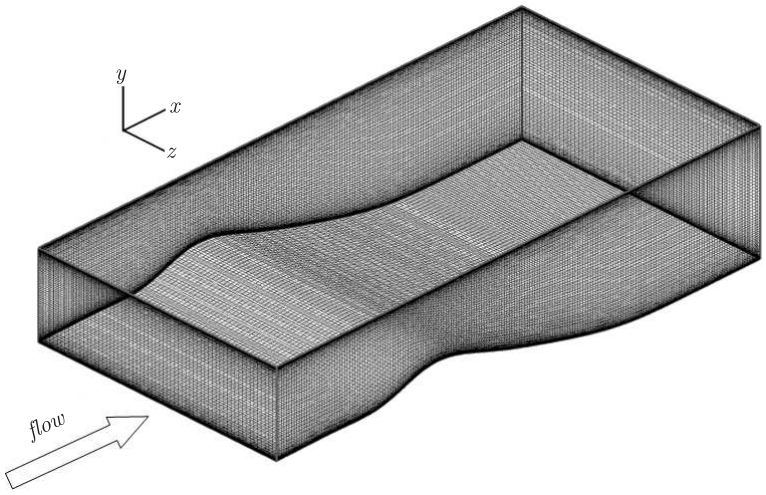

Figure 9. Computational domain of channel with geometry corresponding to the turbomachinery conditions

The simulations were performed at the Reynolds number of $\mathrm{Re}_\tau = 395$ at inlet, which means that a direct comparison (experiment vs. LES) cannot be performed. The only quantity which can be compared is the pressure field. The pressure coefficient C_p distributions at the upper wall and the lower wall of the channel are presented in Figure 10. The black dots correspond to the experimental data (available only for the upper flat plate) and the lines present the current LES

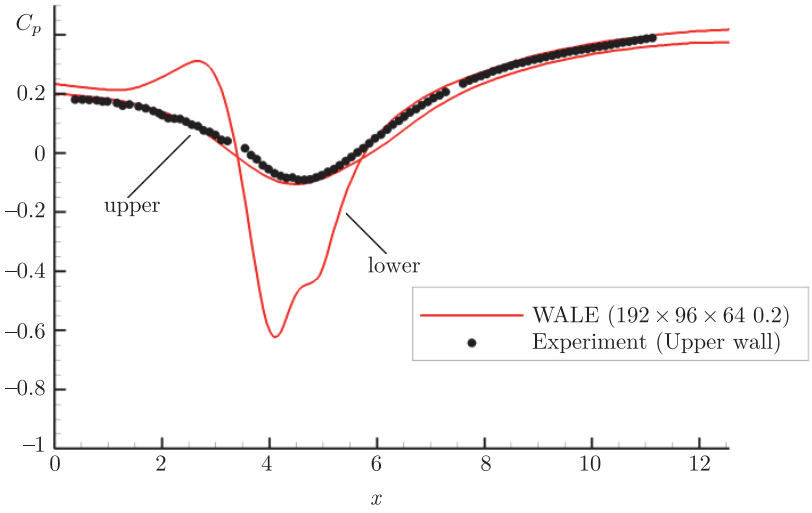

Figure 10. Comparison of the pressure distribution along the domain. LES and experimental results

results. One may notice good agreement between the numerical simulation and the experimental results. In contrast to the LML case, the pressure coefficient increases over 0 at the outlet of the domain which is a direct effect of the change of the cross-section area at the channel outlet.

Figure 11 shows the instantaneous fields of velocity for all three components for the WALE subgrid model with the model constant equal to 0.2. The maximum streamwise velocity reaches 24m/s at the top of the bump. The negative streamwise velocity in the recirculation zone reaches −8m/s, but it is clear that this happens in a very small region. In terms of the wall-normal component, an increase in velocity is observed just before the bump which is a direct reason for the change of the channel cross-section area. Going further, a large scale of wall-normal velocities are observed in the area located after the reattachment point. Similar behavior is observed for the spanwise velocity component, where imprints of large structures are noticed. The scale of these structures increases with the distance from the reattachment point.

In Figure 12 the skin friction distributions for WALE and Smagorinsky subgrid models are presented. The results obtained with two different models are very close to each other in the zero and favorable pressure gradient region, but in the APG region starting from $x = 4$ an apparent discrepancy is observed. It is seen that for the Smagorinsky model the C_f distribution on the lower wall is smeared out and does not show the center of recirculation zone at all (C_f minimum). The shift of C_f is also seen in the upper flat wall. This confirms that the Smagorinsky model does not work properly not only in the recirculation zone but also in the APG flow. Nevertheless, the results do not differ significantly from the WALE model outside this area.

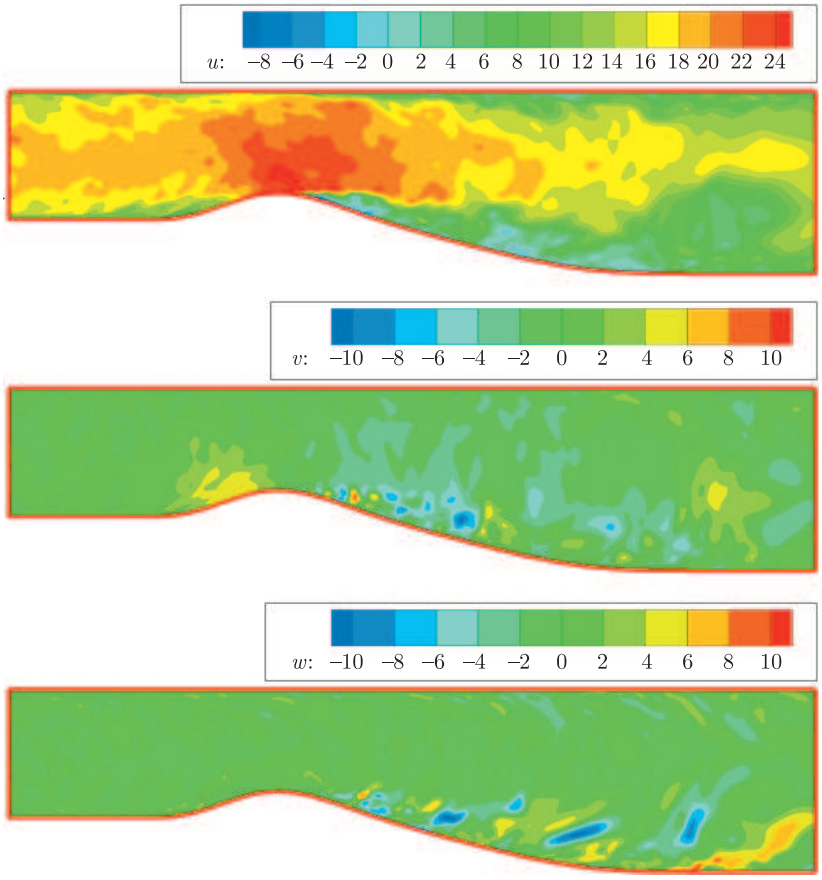

Figure 11. Instantaneous distribution of velocity field (WALE)

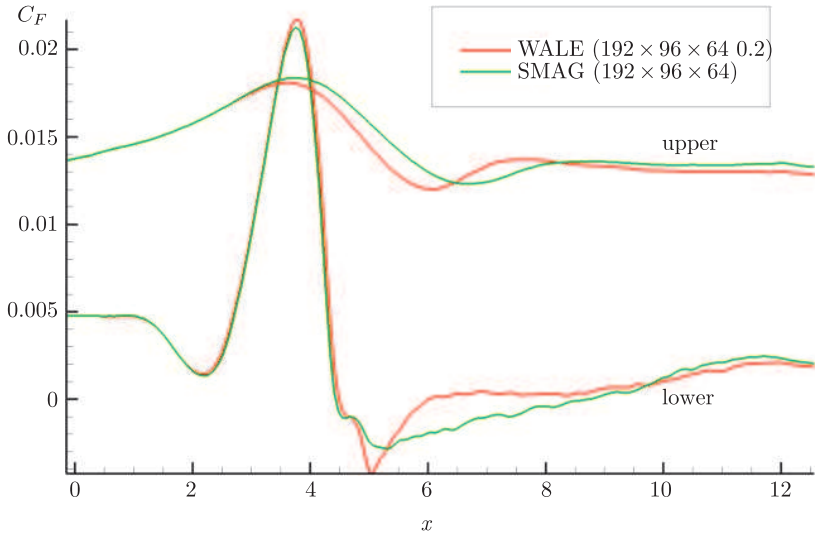

Figure 12. Skin friction coefficient distribution for two different subgrid models

4. Conclusions

The high-order computational code was successfully validated against the DNS data of the LML test section. The comparison with the FDNS results showed good agreement and indicated that using a high order code allows obtaining good results with a relatively coarse mesh. The influence of the subgrid models on the results was analyzed and the optimal model and model constant were indicated. Furthermore, a computational code was applied to simulate the channel flow with the geometry corresponding to the turbomachinery test section of the Czestochowa University of Technology. The obtained results of pressure distribution were in agreement with the experimental data. The performed analysis shows the predictive features of the LES technique for simulation of APG flows.

Acknowledgements

The research was supported by the Polish State Committee for Scientific Research under statutory funds BS-03-301/98.

References

[1] Meyers J, Geurts B J and Baelmans M 2003 *Physics of Fluids* **15** (9) 2740
[2] Meyers J, Geurts B J and Sagaut P J 2007 *J. Comp. Physics* **227** (1) 156
[3] Piomelli U, Moin P and Ferziger J 1988 *Physics of Fluids* **31** 1884
[4] Wu X and Squires K D 1998 *J. Fluid Mech.* **362** 229
[5] Webster D R, Degraaff D B and Eaton J K 1996 *J. Fluid Mech.* **320** 53
[6] El-Askary W A 2010 *Int. J. Num. Methods*, doi: 10.1002/fld.2255
[7] Marquilli M, Laval J P and Dolganov R 2008 *J. Turbulence* **9** (1) 1
[8] Nicoud F and Ducros F 1999 *Turbulence and Combustion* **62** 183
[9] Fletcher C A J 1991 *Computational Techniques for Fluid Dynamics*, Springer-Verlag
[10] Lele S K 1991 *J. Comp. Physics* **103** 16
[11] Laval J P, Elsner W, Kuban L and Marquillie M 2008 *LES Modeling of Converging Diverging Turbulent Channel Flow*, *Proc. Workshop – Progress in Wall Turbulence: Understanding and Modelling*, Lille, France
[12] Materny-Latos M, Drozdz A, Drobniak S and Elsner W 2008 *Arch. Mech.* **60** (6) 1